Volume 8, Issue 4, 2019, 704 - 710 **ISSN 2284-6808**

Letters in Applied NanoBioScience

https://nanobioletters.com/

https://doi.org/10.33263/LIANBS84.704710

Original Research Article **Open Access Journal**

Received: 02.09.2019 / Revised: 18.10.2019 / Accepted: 22.10.2019 / Published on-line: 28.10.2019

Preparation of metal doped quercetin nanoparticles, characterization and their stability study

Siva Mathiyalagan [1], Badal Kumar Mandal [1,*]

[1]Trace Elements Speciation Research Laboratory, Department of Chemistry, School of Advanced Sciences, Vellore Institute of Technology, Vellore- 632014, India

*corresponding author e-mail address: ***badalmandal@vit.ac.in*** | Scopus ID: 7102080708

ABSTRACT

The purpose of this study was to develop metal-loaded (Zn, Cu) quercetin nanoparticles (M-QNPs) using a nanoprecipitation method for the investigation of solubility and stability of QNPs and their metal doped NPs (M-QNPs) in acidic condition. The QNPs and M-QNPs were characterized by using UV-visible and FT-IR spectroscopy, X-ray diffraction, UPLC-DAD, scanning electron microscopy (SEM) and energy dispersive X-ray (EDAX) analysis. The XRD and SEM results of QNPs showed the conversion of the amorphous state of the drug to the crystalline state. The microscopic results demonstrate that the QNPs and M-QNPs showed rod shaped structure which ascribed to a different degree of solubility and stability. In conclusion, the metal doped QNPs improved its stability in acidic condition, but the solubility of M-QNPs was better than that of QNPs which could be used as trace elements supplement for micro-nutrient.

Keywords: *Quercetin nanoparticles (QNPs); metal doped quercetin nanoparticle (M-QNP); solubility, stability.*

1. INTRODUCTION

Solubility plays a major role in drug therapy during administration and hence developing a new pharmaceutical drug with improved solubility is becoming a big challenge to the chemists and pharmacists. About 50-60% of the active pharmaceutical ingredients (APIs) being identified are insoluble or possess low solubility in aqueous medium [1]. The drugs bioavailability of this category is limited due to its low solubility and stability. Wide range of drug formulation development methodologies has been studied extensively to enhance the rates of dissolution of these drugs. One of the advanced modern formulation approach is to reduce the size of the drug particles i.e. to prepare microparticles or nanoparticles of these drugs [2]. Reducing the particle size leads to increases in surface area to volume ratio which improves the dissolution and solubility rate of low water-soluble molecules as well as it also increases bioavailability.

Quercetin ($C_{15}H_{10}O_7$) is a naturally abundant flavonoid in most of the fruits and vegetables (black chokeberry, caper, onion, lettuce and tomato) which are featured in human dietary food. Some study has reported the dietary consumption of this flavonoid as 20-50 mg/day [3]. Due to its high therapeutic efficacy i.e. anti-carcinogenic, antioxidant, antiviral, anti-obesity, anti-inflammatory and antibacterial effects quercetin has been considered as an efficient API in medical industry. Conklin, K. A. (2000) reported the anticancer activity of quercetin which is substantially related to its antioxidant activity and hence it has been included as a nutraceutical ingredient in many food and pharmaceutical industries [4]. It is observed that oxidation and degradation of quercetin lead to the low content of quercetin in food during processing and storage. Also, the stability of quercetin in different food matrix is influenced by temperature, pH, metal ion, and other components such as glutathione (GSH). However, the major difficulties of efficacy of quercetin are due to chemical instability, poor water solubility as well as short biological half-life in consumable products which reduces its bioavailability and efficacy. Quercetin is lipophilic nature and hence is highly soluble in dimethyl sulfoxide and moderately soluble in ethanol, whereas its water solubility is approximately 10 mg/L at 25°C [5].

It is obvious that the hydration or dehydration during phase transitions may change physicochemical properties of bioactive quercetin. Although such changes in physicochemical properties may have practical importance for water insoluble molecules like quercetin, the knowledge of different crystalline structures on the stability and physicochemical properties of the flavonoids is limited or not available in the literature [6].

Therefore the direct incorporation of quercetin at high level in water based food matrixes is difficult. Normally encapsulation of API for delivery systems is adapted to reduce chemical degradation, whereas various methods i.e. polymeric nanoparticles, microparticles, liposomes, polymer encapsulation, high-pressure homogenization and nano-quercetin are practiced to increase the solubility of quercetin in potent cancer therapy [7, 8]. Although these polymeric compounds are not stable in long term storage, it is highly necessary to find out proper delivery vehicles to increase the solubility and stability of quercetin in biological applications. Quercetin has three feasible competitive chelating sites (5-hydroxy-4-carbonyl, 40-dihydroxyl (catechol) and the 3-hydroxy-4-carbonyl groups) (Scheme 1) which is responsible for potential metal chelation. Quercetin complexation with metal cations are reported (Zn(II), Fe(II), Pb(II), Mo(VI), Fe(III), Cu(II), Co(II), Tb(III), Al(III) etc) in literature [9] which is considered as the mechanism for antioxidant activity of flavonoids. In addition, it is assumed that metal chelation with quercetin can influence its stability, solubility, antioxidant and biological effects. Moreover, quercetin being a free radical acceptor shows increased biological activity. As a result, the stability of metal-quercetin complex is

increased, but its solubility in water is not in the satisfactory range. Many researchers tried to improve solubility of quercetin in water by complexation with poly-D, L-lactide (PLA), liposomes and calcium phosphate quercetin nanoparticles (CPQP) [10, 11] and consequently its therapeutic efficacy and bioavailability was increased.

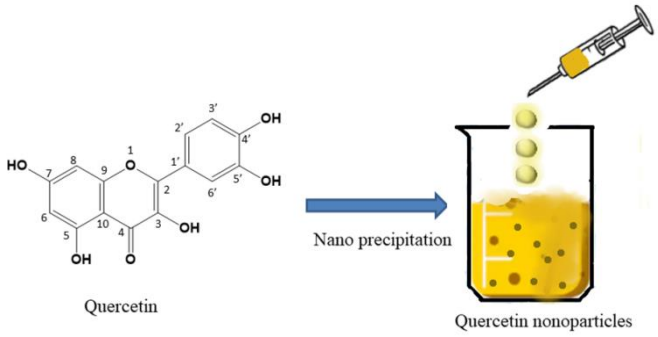

Scheme 1. Schematic representation for the preparation of QNPs from standard Quercetin.

Nanosuspensions are the stabilized colloidal dispersions of nanoparticles produced by appropriate method with selective stabilizer. It is observed that decreasing to nano-size improves the solubility of drug molecules due to the enlarged surface area and saturation solubility as well as dissolution velocity due to increasing vapor pressure of the particles [12]. The hydrophobic drugs like Itraconazole, Ketoconazole, Nebivolol, Amphotericin B, Carbamazepine, Naproxen, Nimesulide, Mitotane, Clotrimazole, Omeprazole, Nifedipine, Spironolactone, Bupravaquone, Bifonazole etc. are formulated as nano-suspension which emerged as a very essential tool in drug delivery to overcome these solubility issues. There are several conventional strategies to improve the solubility of poorly soluble drugs, which include solubilisation, micronization, precipitation technique, co-solvents, permeation enhancers and use of surfactant dispersions. Other techniques are like emulsions, microemulsion liposomes, inclusion complexation and solid dispersion using cyclodextrin. However they lack global relevancy to all drugs. These methodologies are useful for those drugs soluble in organic and aqueous medium. Nanotechnology principles have been used nowadays to solve the problems related to solubility and bioavailability by using conventional methods as well as enhancement. Also, a nanosuspensions are favored over conventional methods for compounds that are not soluble in water but are soluble in high boiling point oil phase [13].

The objectives of the present study were to synthesize novel metal doped quercetin nanoparticles (M-QNPs) by a simple nanoprecipitation method, physicochemical characterization of QNPs and M-QNPs by using Fourier transform infrared spectroscopy (FT-IR), Scanning electron microscopy (SEM), powder X-ray diffraction (XRD), and dissolution study. Finally, the solubility and stability of standard quercetin and the synthesized M-QNPs were monitored by UV-Vis spectroscopy and UPLC equipped with PDA detector.

2. MATERIALS AND METHODS

2.1. Materials.

Extra pure ethanol (HPLC grade), quercetin.2H_2O [2-(3, 4-dihydroxyphenyl)-3,5,7-trihydroxy-4H-1-benzopyran-4one], magnesium sulfate, zinc sulfate, DPPH (2,2-diphenyl-1-picryhydrazyl) were purchased from Sigma Aldrich Chemical Co., Bengaluru, India. All other reagents and solvents were of analytical reagent grade.

2.2. Synthesis of quercetin nanoparticles (QNP).

Quercetin nanoparticles (QNPs) were synthesized by anti-solvent nanoprecipitation technique. Exactly the predetermined concentration of 1 mg Quercetin/mL methanol was used to dissolve commercial quercetin in water for QNPs preparation. A syringe pump was filled with methanol solution of quercetin (1 mg/mL) and the quercetin solution was quickly injected into the deionized water (anti-solvent) of 500 mL at the flow rate of 10 mL/min under magnetic stirring (3000 rpm). The pale yellow precipitate was formed and after 6 h of steadying the QNPs was filtered and vacuum dried.

2.3. Solubility measurements.

The solubility of the QNPs and metal doped QNPs in aqueous solution were quantified by using UV-Vis spectroscopy (JASCO UV-Visible Spectrometer (V-750 PC)) at room temperature. Standard quercetin solutions were prepared in ethanol at various concentrations (1, 5, 9, 11 and 15 mg/L) and the absorbance of each solution was measured at a λ_{max} of 367 nm by using UV-vis spectrophotometer. Then, a saturated solution of QNPs in ethanol was prepared by shaking well for 15 min, centrifuged at 3500 rpm and filtered with a 0.22 mm filter paper to measure its solubility by measuring absorbance with a UV-Vis spectrophotometer. The concentration of the saturated ethanolic QNPs solution was determined from the linear regression equation of the calibration curve.

2.4. X-ray diffractometer (XRD).

The XRD patterns of quercetin and metal doped QNPs were obtained by using X-ray diffractometer (Bruker D8, India.). The powder XRD analysis was performed at a voltage of 40 kV and 25 mA with Cu Kα radiation (λ=1.54 Å, scanning range (2θ value) of 10° to 90°, scanning rate of 4° /min and step size of 0.02°).

2.5. Fourier Transform Infrared (FT-IR) Analysis.

The presence of functional groups in both the synthesized QNPs and M-QNPs was identified by using JASCO FT-IR 4100 (Shimadzu IR AFFINITY-1) in the diffuse reflectance mode at a resolution of 4 cm^{-1}.

2.6. SEM-EDX.

The QNPs powder was dispersed in 1.0 mL deionized water. Then SEM samples were prepared by placing drops on Cu grid followed by drying in a vacuum. The Cu grid was used for the SEM analysis. The morphology of QNPs and M-QNPs were studied using a scanning electron microscope (ZEISS EVO-MA 10, Oberkochen, Germany).

2.7. Stability study of QNPs and M-QNPs.

The stability of QNPs and M-QNPs (M=Zn, Cu) was performed by using UPLC-PDA analysis. The chromatographic analysis was carried out by UPLC-PDA equipped with a pump Quaternary solvent manager auto sampler- sample manager FTN, and PDA-E-LAMBDA detector. The used analytical column was Acquity UPLC BEH C 18 (150mm×2.1mm i.d., 130 Å, 1.7µm) at 37°C. The mobile phase was composed of 0.01 M ammonium acetate buffer and acetonitrile (50:50 v/v), and pH was adjusted to 4.2 with hydrochloric acid. The flow rate was set at 0.7 mL/min. The

samples were prepared in ethanol like UV-vis analysis after proper dilution. The calibrated standards were 10, 30, 50, 70 and 100 mg/L of quercetin which were prepared from ethanolic quercetin solution.

2.8. Yield and encapsulation efficiency.

To calculate the yield of QNPs, the required amount of each sample was dissolved in ethanol and the concentration QNP was quantified by UPLC method. Also, the encapsulation efficiency of metals on the QNPs was performed based on the modified procedure [14]. In brief, the initial concentration of Quercetin was determined before addition of metal ions. Then, the metal doped Quercetin NPs was synthesized after addition of metals ions which were insoluble in ethanol and were removed from ethanol solution by centrifugation and filtration. Finally, the concentration of Quercetin in the filtrate was quantified as earlier. The metal encapsulation efficiency on QNPs and yield were calculated using the given equations (1) and (2):

Encapsulation efficiency (%) = $(C_Q V_Q)-(F_Q V_Q)/ C_Q V_Q$ x 100 ……. (1)

Yield (%) = C_Q x V_Q/W_Q x 100 …….. (2)

Where C_Q is concentration of quercetin in ethanol without metal ions; W_Q is the theoretical amount of quercetin added during the preparation of QNPs; V_Q is the volume of ethanolic dispersion; F_Q is the concentration of quercetin in the filtrate after addition of metal ions.

3. RESULTS

In this study, we have successfully synthesized rod shaped quercetin nanoparticles (QNPs) and the metal doped QNPs (M-QNPs) by nanoprecipitation method. The formation of QNPs was confirmed initially by slow color change of the ethanol solution from dark yellow to light yellow after precipitation of QNPs [15, 16]. QNPs was doped with Cu and Zn metals and rod shaped M-QNPs (M = Zn, Cu) were formed. The FT-IR spectra of quercetin and QNPs were presented in Fig. 1. The QNPs spectra showed two absorption broad bands between 3250 and 2750 cm^{-1} (Fig. 1a and 1b). In most flavonols and flavones like quercetin showed two absorption bands at 237 nm and 358 nm in the UV–Vis region [17]. UV-Vis spectroscopic study of standard flavonoid quercetin, QNPs and M-QNPs showed two major peaks at UV-vis region due to complexation between carbonyl ring C and ring A (benzoyl System). The cinnamoyl group of quercetin was appeared at 300-400 nm (band II), while carbonyl ring C and nearby conjugated ring B showed an absorption band (band I) at 240-300 nm in UV region. Molecular structure of quercetin inferred that it could form complex with metal ions through 3', 4'-dihydroxy and 3-hydroxy-4-oxo system [18, 19]. When metal sulfate solution was added to methanolic solution of quercetin, a significant difference in quercetin spectrum was observed due to the appearance of a new peak at 427 nm [20].

When methanolic quercetin solution was added to water containing polyethylene glycol (PEG) using syringe, band I gradually shifted to a longer wavelength with a decreased absorption value and a new peak appeared at about 400-450 nm which might be associated to the formation of the QNPs [21]. Our FT-IR and UV-Vis analysis results clearly have demonstrated that metal ions were successfully doped onto QNPs by the modified nanodispersion method adopted in this study. Scanning electron microscope was utilized to see the structural and morphological features of the synthesized QNPs and M-QNPs. Generally due to hydrophobic/hydrophilic forces in water nanoparticles tend to aggregate spontaneously in aqueous solutions [22, 23] and hence the formation of these small domains may arise from the aggregation of QNPs. To overcome this formation QNPs aggregate PEG was used as a surfactant to minimize/nullify aggregation of GNPs in aqueous medium. To evaluate the nanostructure of QNPs, XRD analysis was performed to get detailed information about the surface morphology, phase purity and crystallinity of QNPs and M-QNPs (Fig. 2). Some reports informed the existence of anhydrous and dihydrate nature of quercetin and XRD analysis was done for in-depth information on both morphological and surface properties of quercetin [24, 25]. XRD pattern of QNPs is shown in Fig. 2a and the average crystalline size (D) of QNPs was calculated using Scherrer formula: $D=0.9\lambda/\beta \cos\theta$, Where λ= wavelength of X-ray radiation source (1.5406 A°), K = Scherer constant value as 0.9 for spherical particles, β=line width at half maximum high intensity (111) peak. The QNPs were rod shaped with a diameter of 18.2 nm (Fig. 2a) whereas the diameter of standard quercetin was calculated as 40.3 nm (Fig. 2d). Similarly, the diameter of Cu-QNPs and Zn-QNPs were 21.1 nm and 22.6 nm which are comparable to QNP, but are smaller than standard quercetin (Fig. 2).

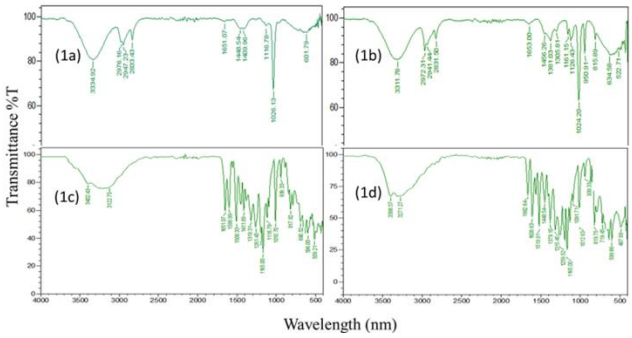

Figure 1. FT-IR spectra of standard Quercetin (1a), QNPs (1b), Zn-QNPs (1c) and Cu-QNPs (1d).

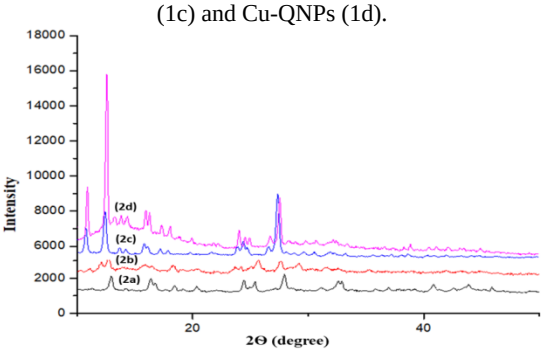

Figure 2. XRD diffractograms of QNP (2a), Zn-QNPs (2b) and Cu-QNPs (2c) and standard Quercetin (2d).

The representative X-ray diffraction patterns of the synthesized QNPs and M-QNPs are shown in Fig 2a-2d. The XRD pattern of the QNPs powder showed the presence of various distinct sharp peaks at 2θ (10.7414°, 11.5046°, 13.8028°, 14.2588°, 15.9411°, 17.5533°, 24.4691° and 27.4290°) which implied crystalline nature of QNPs [26]. The prepared M-QNPs also showed the quite similar peaks but the peaks intensities were slightly less. The Zn-QNPs showed peaks at 2θ (11.1084°, 12.4012°, 12.6803°, 14.2083°, 14.6068°, 16.0944°, 16.6714°, 18.6049°, 20.1795°,

20.8240°, 23.2009°, 26.1010°, 27.9646° and 28.5614°) and Cu-QNPs at 2θ (12.5593°, 14.5891°, 16.4706°, 18.2951°, 20.1011°, 20.9422°, 24.8340°, 25.3622°, 25.4628° and 28.2511°) which implies crystalline nature of these M-QNPs (M = Zn, Cu), respectively. 2θ values of standard quercetin were (10.7212°, 11.5117°, 13.8028°, 14.2588°, 15.9411°, 17.5533°, 24.4691° and 27.4290°) (Fig. 2d).

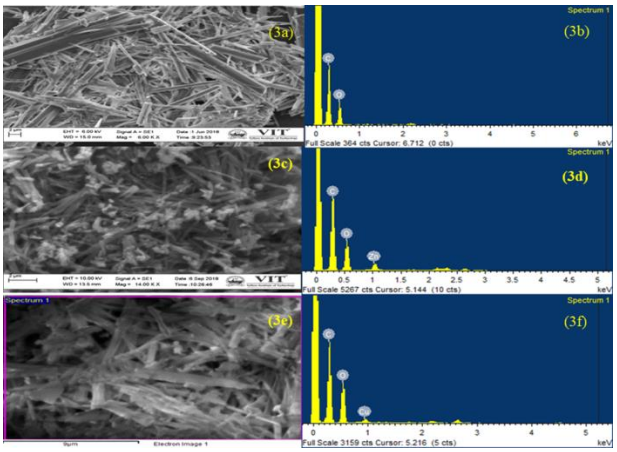

Figure 3. SEM micrographs of QNP (3a), Zn-QNP (3c), Cu-QNP (3e) and EDAX spectra of QNP (3b), Zn-QNP (3d) and Cu-QNP (3f).

The above results suggest that QNPs prepared by nanoprecipitation method appeared no significant changes in crystal structure from its bulk counterpart. The M-QNPs (M = Cu, Zn) also showed similar peaks but the peak intensities of metal doped QNPs decreased [27, 28]. In addition, no significant effect of solvent/anti-solvent ratio, concentration, flow rate and stirring speed on the samples prepared by the syringe pump was found on crystalline structure of QNPs [29]. Noticeably it was found that the QNPs were more crystalline in nature when water was used as an anti-solvent compare to any organic solvents [30]. However, it is difficult to determine the differences in the morphology and particle size caused by changes in the crystal growth conditions or the pseudo-polymorphism i.e. degree of nature of the crystallization solvent, rate of cooling, speed of solution agitation, supersaturation or presence of impurities [31].

In addition, the uniform distribution of rod shaped QNPs on the surface was confirmed by SEM (Fig. 3a). Also, SEM micrographs of Cu-QNPs (Fig. 3c) and Zn-QNPs (Fig. 3e) confirmed the uniform distribution of copper and zinc atoms on the rod-shaped QNPs. The energy-dispersive X-ray (EDAX) analysis is done to find out the elemental composition of QNPs and M-QNPs. EDAX spectrum (3b) of QNPs showed the presence of oxygen and carbon, while EDAX spectra of M-QNPs (M=Cu, Zn) showed the presence of carbon and oxygen with zinc (3d) and copper (3f) respectively, which confirmed the absence of any other impurities in the synthesized QNPs and M-QNPs.

Previous research has claimed that the solubility of quercetin is an essential factor for its bioavailability. For instance, quercetin dissolved in DMSO/polyethylene glycol had bioavailability in rats up to 1.3 fold compared with that suspended in 0.7% carboxymethyl cellulose (CMC) solution [32]. Quercetin bioavailability was improved up to 5.7 fold by a solid lipid nanoparticle as an oral delivery carrier compares to those administered as a quercetin suspension [33].

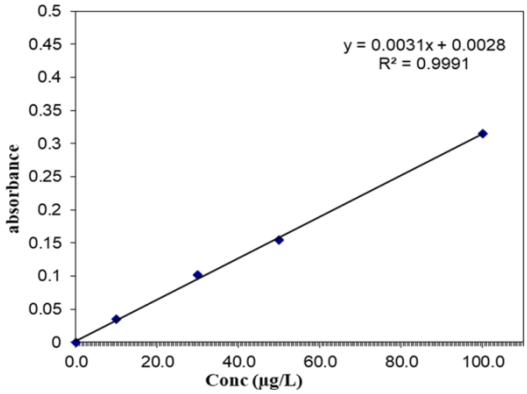

Figure 4. Calibration graph of standard quercetin using UV-Vis spectroscopy.

In this study the solubility of ethanolic quercetin solution was measured by UV-vis analysis. Initially a calibration graph was plotted (Fig. 4) and the calibration graph of quercetin was linear (r^2 = 0.9999) within a range of 1–100 mg/mL. Then the quantity of quercetin in QNPs dispersion in water was checked by UV-vis spectroscopy (Fig. 5) and it was found that solubility of QNPs dispersion was higher than that of standard quercetin in water [std. quercetin = 1.78 mg/L (Fig. 5a) and QNPs =19.41 mg/L (Fig. 5b)]. The stability of quercetin mainly depends on its chemical structure. For instance, the hydroxyl groups present in quercetin molecule (C3, C5, C7, C′4 and C′5) leads to instability. Hence molecular geometry of flavonoid such as quercetin was varied due to the existence of water of hydration into the crystal lattice. Specifically, the crystalline form of quercetin differs according to the hydrogen bonding pattern. Therefore for the anhydrous form, their solubility in water is also diminished. Also, the existence of hydroxyl groups in C3-OH, C′3-OH and C′4-OH positions in conjunction with a C2, C3 double bond are responsible for the antioxidant property of quercetin [34, 35].

The lower pH value has an important influence on the stability of quercetin. A study reported susceptibility of plant phenolic compounds on pH change [36]. Quercetin in aqueous acidic solutions shows instability, which results in loss of concentration (i.e., degradation). The degradation of quercetin involves oxidation, hydroxylation and ring-cleavage. The solubility of M-QNPs (M = Cu, Zn) in ethanol at different pHs are presented in Fig. 6 and Table 1. It clearly shows that Cu-QNPs solution was stable up to 55.1% and Zn-QNPs solution was stable up to 56.2% compare to QNP stability (44.6%) at pH 2.0 (Fig. 6a), whereas Cu-QNPs solution was stable up to 95.7% and Zn-QNPs solution was stable up to 96.8% compare to QNPs stability (97.1%) at pH 6.8 (Fig. 6b). Hence the metal doped QNPs showed higher solubility than QNPs at gastric environment (Fig. 6).

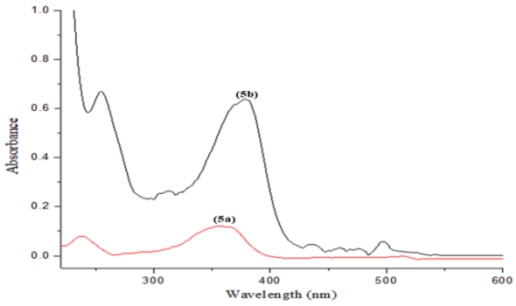

Figure 5. UV-Vis spectra of standard quercetin solution (5a) and QNPs dispersion (5b) in water.

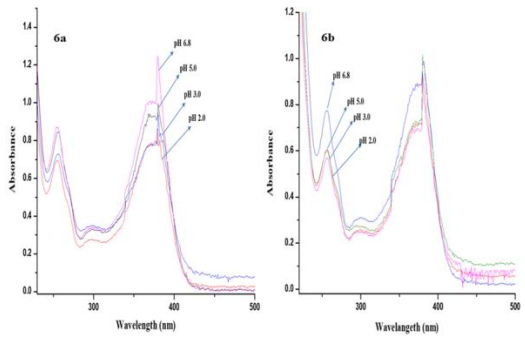

Figure 6. UV-Vis spectra of Cu-QNPs (6a) and Zn-QNPs (6b) in ethanol at different pH.

Also, in the present study the stability of standard quercetin and QNPs were checked by UPLC-PDA analysis after dissolving both standard quercetin and QNPs in ethanol at different pHs (2-6.8) considering gastric pH i.e. biological fluid pH. The solubility of QNPs in ethanol at different pHs is presented in Fig.7 and Table 2. It clearly shows that QNPs solution was stable up to 44.6% compare to quercetin stability (20.8%) at pH 2.0, whereas QNPs solution was stable up to 97.1% compared to quercetin stability (99%) at pH 6.8. It is clear that stability of QNPs was higher at gastric pH i.e. its bioavailability would be higher than standard quercetin in GI tract via oral doses forms. Also, some reports checked the thermal stability of quercetin under different pH. The thermal stability of quercetin solution was evaluated at 100 °C by varying pH 5.0 to pH 8.0 and it was observed that quercetin was more unstable at alkaline pH 7 [37]. This study supported our findings i.e. QNPs were more stable under acidic conditions, especially in gastric environment compare to standard quercetin (Table 1). Previous studies demonstrated that the QNPs had improved solubility rate and antioxidant property [38]. In the present study the identification and confirmation of quercetin i.e. the specificity was performed by the comparison of the peak retention time of quercetin (RT = 3.16 min) with QNPs (RT = 3.2 min). No interference was detected, since no peak was detected in the same retention time of quercetin [Fig. 7] which allows a rapid determination of the drug in different samples. This chromatographic method can help to check the shelf-life of QNPs in different products during storage at different pH and temperature. The major loss of initial quercetin content at pH 2.0 was 45.4% at room temperature. Hence, in order to guarantee stability i.e. shelf-life of quercetin during storage it would be kept under physiological pH or slightly acidic conditions for prolonged periods of shelf-life.

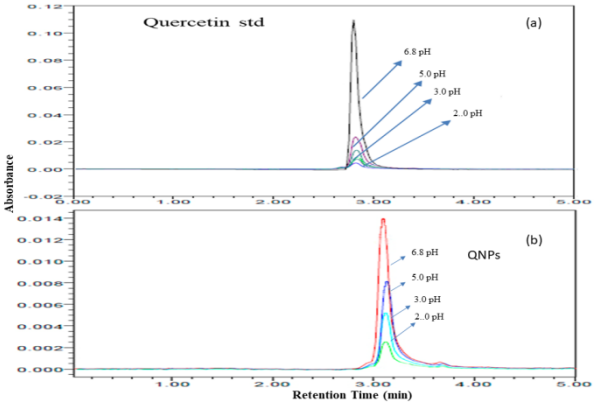

Figure 7. UPLC-PDA chromatograms of standard quercetin (a) and QNPs (b) at different pH.

Table 1. Stability of Cu-QNP and Zn-QNPs at various pH in ethanol using UV-Vis spectroscopy

S.no	Sample conc (ppm)	pH	Cu-QNPs (ppm)	Leftover solubility (%)	Zn-QNPs (ppm)	Leftover solubility (%)
1	20	6.8	19.13	95.7	19.36	96.8
2	20	5.0	17.43	87.2	12.69	63.5
3	20	3.0	11.20	56.0	12.51	62.6
4	20	2.0	11.01	55.1	11.23	56.2

Table 2. Stability of standard quercetin and QNPs in ethanol at different pH by UPLC-PDA analysis.

S.no	Sample conc. (ppm)	pH	Quercetin (ppm)	Leftover solubility (%)	QNPs (ppm)	Leftover solubility (%)
1	20	6.8	19.80	99	19.41	97.1
2	20	5.0	11.04	55.2	17.26	86.3
3	20	3.0	5.91	29.6	13.01	65.1
4	20	2.0	4.16	20.8	8.94	44.6

4. CONCLUSIONS

The present study demonstrated that the solvent/anti-solvent precipitation process successfully produced QNPs with the smaller particle size using a nanoprecipitation method. Our studies also established that the dissolution of quercetin was enhanced due to the reduction of quercetin particle size. Additionally, the stability of M-QNPs from QNP improved physicochemical characterization and dissolution property. Thus, we suggest that the QNPs could be applied in clinical settings as well as warrant further studies for a nutrient supplement of beneficial micro-trace elements like Zn and Cu.

5. REFERENCES

1. Rasaie, S.; Ghanbarzadeh, S.; Mohammadi, M.; Hamishehkar, H. Nano phytosomes of quercetin: A promising formulation for fortification of food products with antioxidants. *Pharmaceutical Sciences* **2014**, 20, 96-101.

2. Ravichandran, R.; Rajendran, M.; Devapiriam, D. Antioxidant study of quercetin and their metal complex and determination of stability constant by spectrophotometry method. *Food Chemistry* **2014**, *146*, 472-478, http://doi.org/10.1016/j.foodchem.2013.09.080.

3. Nishimuro, H.; Ohnishi, H.; Sato, M.; Ohnishi-Kameyama, M.; Matsunaga, I.; Naito, S.; Saitoh, S. Estimated daily intake and seasonal food sources of quercetin in Japan. *Nutrients* **2015**, *7*, 2345-2358, http://doi.org/10.3390/nu7042345.

4. Ruchi, S. Role of nutraceuticals in health care: A review. *International Journal of Green Pharmacy (IJGP)* **2017**, *11*, http://dx.doi.org/10.22377/ijgp.v11i03.1146
5. Fang, R.; Hao, R.; Wu, X.; Li, Q.; Leng, X.; Jing, H. Bovine serum albumin nanoparticle promotes the stability of quercetin in simulated intestinal fluid. *Journal of Agricultural and Food Chemistry* **2011**, *59*, 6292-6298, https://doi.org/10.1021/jf200718j.
6. Borghetti, G.S.; Carini, J.P.; Honorato, S.B.; Ayala, A.P.; Moreira, J.C.F.; Bassani, V.L. Physicochemical properties and thermal stability of quercetin hydrates in the solid state. *Thermochimica Acta* **2012**, *539*, 109-114, https://doi.org/10.1016/j.tca.2012.04.015.
7. Bonifacio, B.V.; da Silva, P.B.; dos Santos Ramos, M.A.; Negri, K.M.S.; Bauab, T.M.; Chorilli, M. Nanotechnology-based drug delivery systems and herbal medicines: a review. *International Journal of Nanomedicine* **2014**, *9*, 1, http://doi.org/10.2147/IJN.S52634.
8. Din, F.U.; Saleem, S.; Aleem, F.; Ahmed, R.; Huda, N.U.; Ahmed, S.; Aman, W. Advanced colloidal technologies for the enhanced bioavailability of drugs. *Cogent Medicine* **2018**, *5*, 1480572, https://doi.org/10.1080/2331205X.2018.1480572.
9. Zhou, J.; Wang, L.; Wang, J.; Tang, N. Antioxidative and anti-tumour activities of solid quercetin metal (II) complexes. *Transition Metal Chemistry* **2001**, *26*, https://doi.org/10.1023/A:1007152927167.
10. Bukhari, S.B.; Memon, S.; Mahroof-Tahir, M.; Bhanger, M.I. Synthesis, characterization and antioxidant activity copper–quercetin complex. *Spectrochimica Acta Part A: Molecular and Biomolecular Spectroscopy* **2009**, *71*, 1901-1906, http://doi.org/10.1016/j.saa.2008.07.030.
11. Alam, M.M.; Abdullah, K.M.; Singh, B.R.; Naqvi, A.H.; Naseem, I. Ameliorative effect of quercetin nanorods on diabetic mice: mechanistic and therapeutic strategies. *RSC Advances* **2016**, *6*, 55092-55103, http://doi.org/10.1039/C6RA04821H.
12. Pal, R.; Panigrahi, S.; Bhattacharyya, D.; Chakraborti, A.S. Characterization of citrate capped gold nanoparticle-quercetin complex: Experimental and quantum chemical approach. *Journal of Molecular Structure* **2013**, *1046*, 153-163, http://doi.org/10.1016/j.molstruc.2013.04.043.
13. Lou, M.; Zhang, L.N.; Ji, P.G.; Feng, F.Q.; Liu, J.H.; Yang, C.; Wang, L. Quercetin nanoparticles induced autophagy and apoptosis through AKT/ERK/Caspase-3 signaling pathway in human neuroglioma cells: In vitro and in vivo. *Biomedicine & Pharmacotherapy* **2016**, *84*, 1-9, http://dx.doi.org/10.1016/j.biopha.2016.08.055.
14. Han, Q.; Wang, X.; Cai, S.; Liu, X.; Zhang, Y.; Yang, L.; Yang, R. Quercetin nanoparticles with enhanced bioavailability as multifunctional agents toward amyloid induced neurotoxicity. *Journal of Materials Chemistry B* **2018**, *6*, 1387-1393, http://doi.org/10.1039/C7TB03053C.
15. Wu, T.H.; Yen, F.L.; Lin, L.T.; Tsai, T.R.; Lin, C.C.; Cham, T.M. Preparation, physicochemical characterization, and antioxidant effects of quercetin nanoparticles. *International Journal of Pharmaceutics* **2008**, *346*, 160-168, https://doi.org/10.1016/j.ijpharm.2007.06.036.
16. Patra, M.; Mukherjee, R.; Banik, M.; Dutta, D.; Begum, N.A.; Basu, T. Calcium phosphate-quercetin nanocomposite (CPQN): A multi-functional nanoparticle having pH indicating, highly fluorescent and anti-oxidant properties. *Colloids and Surfaces B: Biointerfaces* **2017**, *154*, 63-73, http://doi.org/10.1016/j.colsurfb.2017.03.018.
17. Cornard, J.P.; Dangleterre, L.; Lapouge, C. Computational and spectroscopic characterization of the molecular and electronic structure of the Pb(II)–quercetin complex. *Journal Physical Chemistry A* **2005**, *109*, 10044–10051, https://doi.org/10.1021/jp053506i.
18. Cornard, J.P.; Merlin, J.C.; Boudet, A.C.; Vrielynck, L. Structural study of quercetin by vibrational and electronic spectroscopies combined with semiempirical calculations. *Biospectroscopy* **1997**, *3*, 183–193, https://doi.org/10.1002/(SICI)1520-6343.
19. Liu, P.; Zhao, L.; Wu, X.; Huang, F.; Wang, M.; Liu, X. Fluorescence enhancement of quercetin complexes by silver nanoparticles and its analytical application. *Spectrochimica Acta Part A: Molecular and Biomolecular Spectroscopy* **2014**, *122*, 238-245, http://dx.doi.org/10.1016/j.saa.2013.11.055.
20. Hussain, J.; Mabood, F.; Al-Harrasi, A.; Ali, L.; Rizvi, T.S.; Jabeen, F.; Al Ghawi, S.H.S. New robust sensitive fluorescence spectroscopy coupled with PLSR for estimation of quercetin in Ziziphus mucronata and Ziziphus sativa. *Spectrochimica Acta Part A: Molecular and Biomolecular Spectroscopy* **2018**, *194*, 152-157, https://doi.org/10.1016/j.saa.2018.01.002.
21. Ayala, A.P.; Siesler, H.W.; Wardell, S.M.S.V.; Boechat, N.; Dabbene, V.; Cuffini, S.L. Vibrational spectra and quantum mechanical calculations of antiretroviral drugs: nevirapine. *Journal of Molecular Structure* **2007**, *828*, 201–210, https://doi.org/10.1016/j.molstruc.2006.05.055.
22. Rizvi, T.S.; Mabood, F.; Ali, L.; Al-Broumi, M.; Al Rabani, H.K.M.; Hussain, J.; Jabeen, F.; Manzoor, S.; Al-Harrasi, A. Application of NIR Spectroscopy Coupled with PLS Regression for Quantification of Total Polyphenol Contents from the Fruit and Aerial Parts of Citrullus colocynthis. *Phytochemical Analysis* **2018**, *29*, 16-22, https://doi.org/10.1002/pca.2710.
23. Lu, X.; Ross, C.F.; Powers, J.R.; Rasco, B.A. Determination of quercitins in onions (Allium cepa) using infrared spectroscopy. *Journal of Agricultural and Food Chemistry* **2011**, *59*, 6376–6382, http://doi.org/10.1021/jf200953z.
24. Mabood, F.; Jabeen, F.; Ahmed, M.; Al Mashaykhi, S.A.A.; Al Rubaiey, Z.M.A.; Hussain, J.; Harrasi, A.A.; Ali, L. Development of new NIR-spectroscopy method combined with multivariate analysis for detection of adulteration in camel milk with goat milk. *Food Chemistry* **2017**, *221*, 746–750. http://doi.org/10.1016/j.foodchem.2016.11.109.
25. Borghetti, G.S.; Costa, I.M.; Petrovick, P.R.; Pereira, V.P.; Bassani, V.L. Characterization of different samples of quercetin in solid-state: indication of polymorphism occurrence. *Pharmazie* **2006**, *61*, 802–804, http://doi.org/10.1208/s12249-009-9196-3.
26. Olejniczak, S.; Potrzebowski, M.J. Solid state NMR studies and density functional theory (DFT) calculations of conformers of quercetin. *Organic & Biomolecular Chemistry* **2004**, *2*, 2315–2322, http://doi.org/10.1039/B406861K.
27. Khaled, K.A.; El-Sayed, Y.M.; Al-Hadiya, B.M. Disposition of the flavonoid quercetin in rats after single intravenous and oral doses. *Drug Development and Industrial Pharmacy* **2003**, *29*, 397-403, https://doi.org/10.1081/DDC-120018375.
28. Li, H.; Zhao, X.; Ma, Y.; Zhai, G.; Li, L.; Lou, H. Enhancement of gastrointestinal absorption of quercetin by solid lipid nanoparticles. *Journal of Controlled Release* **2009**, *133*, 238-244, https://doi.org/10.1016/j.jconrel.2008.10.002.
29. Friedman, M.; Jürgens, H.S. Effect of pH on the stability of plant phenolic compounds. *Journal of Agricultural and Food Chemistry* **2000**, *48*, 2101-2110, https://doi.org/10.1021/jf990489j.

30. Kırca, A.; Özkan, M.; Cemeroğlu, B. Effects of temperature, solid content and pH on the stability of black carrot anthocyanins. *Food Chemistry* **2007**, *101*, 212-218, http://doi.org/10.1016/j.foodchem.2006.01.019
31. Kumari, A.; Yadav, S.K., Pakade, Y.B.; Singh, B.; Yadav, S.C. Development of biodegradable nanoparticles for delivery of quercetin. *Colloids and Surfaces B: Biointerfaces* **2010**, *80*, 184-192, http://doi.org/10.1016/j.colsurfb.2010.06.002.
32. Vippagunta, S.R.; Brittain, H.G.; Grant, D.J.W. Crystalline solids. *Advanced Drug Delivery Reviews* **2001**, *48*, 3–26, http://doi.org/10.1016/S0169-409X(01)00097-7.
33. Pralhad, T.; Rajendrakumar, K. Study of freeze-dried quercetin–cyclodextrin binary systems by DSC, FT-IR, X-ray diffraction and SEM analysis. *Journal of Pharmaceutical and Biomedical Analysis* **2004**, *34*, 333–339, http:///doi.org/10.1016/S0731-7085(03)00529-6.
34. Landim, L.P.; Feitoza, G.S.; da Costa, J.G.M. Development and validation of a HPLC method for the quantification of three flavonoids in a crude extract of Dimorphandra gardneriana. *Revista Brasileira de Farmacognosia* **2013**, *23*, 58–64, http://doi.org/10.1590/s0102-695x2012005000111.
35. Formica, J.V.; Regelson, W. Review of the biology of quercetin and related bioflavonoids. *Food and Chemical Toxicology* **1995**, *33*, 1061-1080, http://doi.org/10.1016/0278-6915(95)00077-1.
36. Anandam, S.; Selvamuthukumar, S. Fabrication of cyclodextrin nanosponges for quercetin delivery: physicochemical characterization, photostability, and antioxidant effects. *Journal of Materials Science* **2014**, *49*, 8140–8153, https://doi.org/10.1007/s10853-014-8523-6.
37. Scalia, S.; Mezzena, M. Incorporation of quercetin in lipid microparticles: effect on photo- and chemical-stability. *Journal of Pharmaceutical and Biomedical Analysis* **2009**, *49*, 90–94, http://doi.org/10.1016/j.jpba.2008.10.011.
38. Boots, A.W.; Haenen, G.R.M.M.; Bast, A. Health effects of quercetin: from antioxidant to nutraceutical. *European Journal of Pharmacology* **2008**, *585*, 325–337, http://doi.org/10.1016/j.ejphar.2008.03.008.

6. ACKNOWLEDGEMENTS

The authors thank Vellore Institute of Technology, Vellore for the financial support, working platform and instrument facility given to complete the study. Especially, the authors thank Vellore Institute of Technology, Vellore for providing “VIT SEED GRANT” for carrying out this research work.

© 2019 by the authors. This article is an open access article distributed under the terms and conditions of the Creative Commons Attribution (CC BY) license (http://creativecommons.org/licenses/by/4.0/).